

## **Supporting Online Material**

# **Contribution of seasonal sub-Antarctic surface water variability to millennial-scale changes in atmospheric CO<sub>2</sub> over the last deglaciation and Marine Isotope Stage 3**

Julia Gottschalk<sup>1</sup>, Luke C. Skinner<sup>1</sup>, Claire Waelbroeck<sup>2</sup>

Corresponding Author: J. Gottschalk (jg619@cam.ac.uk, +44 (0) 1223 768342)

<sup>1</sup>Godwin Laboratory for Palaeoclimate Research, Department of Earth Sciences, University of Cambridge, Cambridge CB2 3EQ, UK

<sup>2</sup>LSCE/IPSL Laboratoire, CNRS-CEA-UVSQ, 91198 Gif-sur-Yvette, France

Keywords: South Atlantic, planktonic foraminifera, stable oxygen and carbon isotopes, atmospheric CO<sub>2</sub>, last glacial period

## **1. Compilation of South Atlantic core-top $\delta^{18}\text{O}$ and $\delta^{13}\text{C}$ of *G. bulloides* and *N. pachyderma* (s.)**

The planktonic  $\delta^{18}\text{O}$  and  $\delta^{13}\text{C}$  data compilation includes a number of published (Duplessy et al., 1991; Keigwin and Boyle, 1989; Kohfeld et al., 2000; Multizzi et al., 1997; Niebler, 1995; Niebler et al., 1999) and unpublished (Hubberten and Niebler, pers. comm.) data sets. Unpublished data are listed in Table S1.

To minimize a potential bias of the planktonic  $\delta^{18}\text{O}$  and  $\delta^{13}\text{C}$  compilation by size fraction variations (Niebler et al., 1999; Oppo and Fairbanks, 1989), we have omitted data obtained from very small ( $<200\ \mu\text{m}$ ) and very big ( $>315\ \mu\text{m}$ ) size fractions, where documentation for the data was available. The size fractions included in the compilation of planktonic  $\delta^{13}\text{C}$  ( $200\text{-}250\ \mu\text{m}$  and  $250\text{-}315\ \mu\text{m}$ ) are therefore similar to those of our down-core analyses. However, information on the measured size fraction was not available for a large portion of the planktonic  $\delta^{18}\text{O}$  dataset, which may partly explain the large variability of the planktonic  $\delta^{18}\text{O}$  data (Fig. 3). We have therefore calculated a latitudinal ( $2^\circ$ -running) mean (as well as the corresponding  $\pm$ one sigma variability), which reduces the bias likely caused by measurements on different size fractions and allows a comparison to hydrographic data of the proposed modern foraminiferal habitats to be made.

## **2. Age model MD07-3076Q**

Age-depth markers that result from splicing the radiocarbon- and *N. pachyderma* (s.) abundance-based chronologies are given in Table S2. The final chronology is based on a linear interpolation between these tiepoints.

Age uncertainties of the *N. pachyderma* (s.)-based chronology (Fig. S1) may result from the choice of the reference ice core temperature record (e.g. EPICA Dome C (EDC)  $\delta\text{D}$  versus EPICA Dronning-Maud-Land (EDML)  $\delta^{18}\text{O}$ ) and different alignment approaches (tiepoints in maximum versus transitional phases of Antarctic temperature change). We have assessed this uncertainty by calculating the maximum 95% highest posterior density region (Fig. S1) resulting from the individual alignment approaches with the Bayesian statistical software BACHRON (Haslett and Parnell, 2008). The resulting

mean age uncertainty of the *N. pachyderma* (s.) abundance-based chronology amounts to  $1600 \pm 500$  years. The outcome of this study does not depend on the choice of the reference Antarctic temperature record.

### **3. Gas age scales of CO<sub>2</sub> records from Antarctic ice cores**

Deglacial CO<sub>2,atm</sub> data of the BYRD (Neftel et al., 1988; Staffelbach et al., 1991) and Siple Dome (Ahn et al., 2004) ice cores are reported on the GICC05 gas age scale obtained by Pedro et al., (2012). The age scales are based on a methane synchronization of BYRD to the Greenland ice cores (Blunier and Brook, 2001; Brook et al., 2005). The EDC1 age scale of deglacial CO<sub>2,atm</sub> data obtained from the EDC ice core (Monnin et al., 2001) has been converted to the AICC2012 gas age scale using the depth-gas age relation obtained by Veres et al., (2013).

Gas ages of CO<sub>2,atm</sub> reconstructed for the last glacial cycle from BYRD (Ahn and Brook, 2008; Ahn et al., 2012) have been transferred to the AICC2012 age scale by CH<sub>4</sub> synchronization of BYRD and EDML (Blunier and Brook, 2001; EPICA Community Members, 2006), whereby the methane record of EDML has been transferred to the AICC2012 gas age scale according to the depth-gas age constraints of Veres et al., (2013). EDML1\_sc4 gas ages for CO<sub>2,atm</sub> data of the Talos Dome (Bereiter et al., 2012) and EDML (Bereiter et al., 2012; Lüthi et al., 2010) ice cores have been similarly adjusted to AICC2012 gas ages (Veres et al., 2013). The GT4 Vostok age scale of CO<sub>2,atm</sub> data reported from Taylor Dome (Indermühle et al., 2000) have been converted to AICC2012 gas ages according to the depth-gas age constraints in the Vostok ice core by Veres et al., (2013). CO<sub>2</sub> data from the Siple Dome ice core (Ahn and Brook, 2014) are shown on the GICC05 age scale reported by Ahn and Brook, (2014).

The relative timing of the adapted gas age scales of the various CO<sub>2,atm</sub> records has been checked by applying the same gas ages scale to the respective methane records of the BYRD (Blunier and Brook, 2001), Siple Dome (Ahn and Brook, 2014; Brook et al., 2005), EDC (Monnin et al., 2001), EDML (EPICA Community Members, 2006), Taylor Dome (Brook et al., 2000) and Talos Dome (Buiiron et

al., 2012) ice cores. The adjusted gas age scales agree well within centuries (Fig. S2). Mean CO<sub>2,atm</sub> changes have been calculated by averaging all available CO<sub>2,atm</sub> data interpolated on a common, 100 year-spaced time scale (Fig. S2).

#### **4. Correction of planktonic foraminifer δ<sup>13</sup>C**

Planktonic foraminifer δ<sup>13</sup>C (δ<sup>13</sup>C<sub>shell</sub>) have been corrected for the temperature (T), carbonate ion (CO<sub>3</sub><sup>2-</sup>) and dietary (i.e. particulate organic matter, POM) δ<sup>13</sup>C effects according to the procedure outlined in Kohfeld et al., (2000) applying equation 1.

$$\delta^{13}\text{C}_{\text{eq}} = \delta^{13}\text{C}_{\text{shell}} + 0.13 \text{ T} + 0.013 [\text{CO}_3^{2-}] - 0.084 \delta^{13}\text{C}_{\text{POM}} + B_{\text{tot}} \quad (1)$$

An adjustment constant B<sub>tot</sub> of -2.3 and -2.9 has been applied for the corrections of *G. bulloides* and *N. pachyderma* (s.) δ<sup>13</sup>C<sub>shell</sub>, respectively. Our applied B<sub>tot</sub> for correcting *N. pachyderma* (s.) δ<sup>13</sup>C agrees well with the applied value of -2.8 reported by Kohfeld et al., (2000). The stable carbon isotopic composition of the foraminiferal diet has been approximated by δ<sup>13</sup>C of POM reported by Goericke and Fry, (1994). Temperatures used for the correction of *G. bulloides* δ<sup>13</sup>C have been extracted from the World Ocean Atlas 2009 (Locarnini et al., 2010) and are taken to be spring and summer temperatures averaged over the water depth intervals 0-100 m north and south of the PF, respectively. Temperatures to correct *N. pachyderma* (s.) δ<sup>13</sup>C refer to summer surface temperatures averaged over the water levels 0-100 m and 50-150 m north and south of the PF, respectively. Mean annual CO<sub>3</sub><sup>2-</sup> concentrations have been used for the correction of planktonic δ<sup>13</sup>C and have been computed from the GLODAP data set (Key et al., 2004) using the CO<sub>2</sub>SYS program (Lewis and Wallace, 1998). Mean annual CO<sub>3</sub><sup>2-</sup> concentrations averaged over a water depth of 0-100 m have been applied to represent the near-surface habitats of *G. bulloides* and *N. pachyderma* (s.), and CO<sub>3</sub><sup>2-</sup> data averaged over a water depth of 50-150 m has been selected to represent the ‘sub-surface’ habitat of *N. pachyderma* (s.) south of the PF. The temperature and CO<sub>3</sub><sup>2-</sup> data used for the corrections have been obtained along 20°W.

## **References**

- Ahn, J., Brook, E.J., 2008. Atmospheric CO<sub>2</sub> and climate on millennial time scales during the last glacial period. *Science* 322, 83–85. doi: 10.1126/science.1160832
- Ahn, J., Brook, E.J., 2014. Siple Dome ice reveals two modes of millennial CO<sub>2</sub> change during the last ice age. *Nat. Commun.* 5, 3723. doi: 10.1038/ncomms4723
- Ahn, J., Brook, E.J., Schmittner, A., Kreutz, K., 2012. Abrupt change in atmospheric CO<sub>2</sub> during the last ice age. *Geophys. Res. Lett.* 39. doi: 10.1029/2012GL053018
- Ahn, J., Wahlen, M., Deck, B.L., Brook, E.J., Mayewski, P.A., Taylor, K.C., White, J.W.C., 2004. A record of atmospheric CO<sub>2</sub> during the last 40,000 years from the Siple Dome, Antarctica ice core. *J. Geophys. Res. Atmos.* 109. doi: 10.1029/2003JD004415
- Bereiter, B., Lüthi, D., Siegrist, M., Schüpbach, S., Stocker, T.F., Fischer, H., 2012. Mode change of millennial CO<sub>2</sub> variability during the last glacial cycle associated with a bipolar marine carbon seesaw. *Proc. Natl. Acad. Sci.* 109, 9755–9760. doi: 10.1073/pnas.1204069109
- Blunier, T., Brook, E.J., 2001. Timing of millennial-scale climate change in Antarctica and Greenland during the last glacial period. *Science* 291, 109. doi: 10.1126/science.291.5501.109
- Brook, E.J., Harder, S., Severinghaus, J., Steig, E.J., Sucher, C.M., 2000. On the origin and timing of rapid changes in atmospheric methane during the last glacial period. *Global Biogeochem. Cycles* 14, 559–572. doi: 10.1029/1999GB001182
- Brook, E.J., White, J.W.C., Schilla, A.S.M., Bender, M.L., Barnett, B., Severinghaus, J.P., Taylor, K.C., Alley, R.B., Steig, E.J., 2005. Timing of millennial-scale climate change at Siple Dome, West Antarctica, during the last glacial period. *Quat. Sci. Rev.* 24, 1333–1343. doi: 10.1016/j.quascirev.2005.02.002
- Buiron, D., Stenni, B., Chappellaz, J., Landais, A., Baumgartner, M., Bonazza, M., Capron, E., Frezzotti, M., Kageyama, M., Lemieux-Dudon, B., Masson-Delmotte, V., Parrenin, E., Schilt, A., Selmo, E., Severi, M., Swingedouw, D., Udisti, R., 2012. Regional imprints of millennial variability during the MIS 3 period around Antarctica. *Quat. Sci. Rev.* 48, 99–112. doi: 10.1016/j.quascirev.2012.05.023
- Duplessy, J.C., Labeyrie, L., Juillet-Leclerc, A., Maitre, F., Duprat, J., Sarnthein, M., 1991. Surface salinity reconstruction of the North-Atlantic Ocean during the last glacial maximum. *Oceanol. Acta* 14, 311–324.
- EPICA Community Members, 2006. One-to-one coupling of glacial climate variability in Greenland and Antarctica. *Nature* 444, 195–198. doi: 10.1038/nature05301
- Goericke, R., Fry, B., 1994. Variations of marine plankton δ<sup>13</sup>C with latitude, temperature, and dissolved CO<sub>2</sub> in the world ocean. *Global Biogeochem. Cycles* 8, 85–90. doi: 10.1029/93GB03272
- Haslett, J., Parnell, A., 2008. A simple monotone process with application to radiocarbon-dated depth chronologies. *J. R. Stat. Soc. Ser. B Stat. Methodol.* 77, 399–418. doi: 10.1111/j.1467-9876.2008.00623.x
- Indermühle, A., Monnin, E., Stauffer, B., Stocker, T.F., Wahlen, M., 2000. Atmospheric CO<sub>2</sub> concentration from 60 to 20 kyr BP from the Taylor Dome ice core, Antarctica. *Geophys. Res. Lett.* 27, 735–738. doi: 10.1029/1999GL010960

Jouzel, J., Masson-Delmotte, V., Cattani, O., Dreyfus, G., Falourd, S., Hoffmann, G., Minster, B., Nouet, J., Barnola, J.M., Chappellaz, J., Fischer, H., Gallet, J.C., Johnsen, S., Leuenberger, M., Louergue, L., Luethi, D., Oerter, H., Parrenin, F., Raisbeck, G., Raynaud, D., Schilt, A., Schwander, J., Selmo, E., Souchez, R., Spahni, R., Stauffer, B., Steffensen, J.P., Stenni, B., Stocker, T.F., Tison, J.L., Werner, M., Wolff, E.W., 2007. Orbital and millennial Antarctic climate variability over the past 800,000 years. *Science* 317, 793. doi: 10.1126/science.1141038

Keigwin, L.D., Boyle, E.A., 1989. Late Quaternary paleochemistry of high-latitude surface waters. *Palaeogeogr. Palaeoclimatol. Palaeoecol.* 73, 85–106. doi: 10.1016/0031-0182(89)90047-3

Key, R.M., Kozyr, A., Sabine, C.L., Lee, K., Wanninkhof, R., Bullister, J.L., Feely, R.A., Millero, F.J., Mordy, C., Peng, T.-H., 2004. A global ocean carbon climatology: Results from Global Data Analysis Project (GLODAP). *Global Biogeochem. Cycles* 18, GB4031. doi: 10.1029/2004GB002247

Kohfeld, K.E., Anderson, R.F., Lynch-Stieglitz, J., 2000. Carbon isotopic disequilibrium in polar planktonic foraminifera and its impact on modern and Last Glacial Maximum reconstructions. *Paleoceanography* 15, 53–64. doi: 10.1029/1999PA900049

Lewis, E., Wallace, D.W.R., 1998. Program developed for CO<sub>2</sub> system calculations, Oak Ridge, Oak Ridge National Laboratory ORNL/CDIAC-105. Carbon Dioxide Information Analysis Center, Oak Ridge National Laboratory, US Dept. of Energy.

Locarnini, R.A., Mishonov, A. V., Antonov, J.I., Boyer, T.P., Garcia, H.E., Baranova, O.K., Zweng, M.M., Johnson, D.R., 2010. World Ocean Atlas 2009, Volume 1: Temperature, NOAA Atlas NESDIS 68. U.S. Government Printing Office, Washington, D.C.

Lüthi, D., Bereiter, B., Stauffer, B., Winkler, R., Schwander, J., Kindler, P., Leuenberger, M., Kipfstuhl, S., Capron, E., Landais, A., Fischer, H., Stocker, T.F., 2010. CO<sub>2</sub> and O<sub>2</sub>/N<sub>2</sub> variations in and just below the bubble-clathrate transformation zone of Antarctic ice cores. *Earth Planet. Sci. Lett.* 297, 226–233. doi: 10.1016/j.epsl.2010.06.023

Monnin, E., Indermühle, A., Dällenbach, A., Flückiger, J., Stauffer, B., Stocker, T.F., Raynaud, D., Barnola, J.M., 2001. Atmospheric CO<sub>2</sub> concentrations over the last glacial termination. *Science* 291, 112. doi: 10.1126/science.291.5501.112

Mulitza, S., Dürkoop, A., Hale, W., Wefer, G., Niebler, H.S., 1997. Planktonic foraminifera as recorders of past surface-water stratification. *Geology* 25, 335–338. doi: 10.1130/0091-7613(1997)025<0335:PFAROP>2.3.CO;2

Neftel, A., Oeschger, H., Staffelbach, T., Stauffer, B., 1988. CO<sub>2</sub> record in the Byrd ice core 50,000–5,000 years bp. *Nature* 331, 609–611. doi: 10.1038/331609a0

Niebler, H.-S., 1995. Reconstruction of paleo-environmental parameters using stable isotopes and faunal assemblages of planktonic foraminifera in the South Atlantic Ocean. *Berichte zur Polarforsch.* 167, 198.

Niebler, H.-S., Hubberten, H.-W., Gersonde, R., 1999. Oxygen isotope values of planktic foraminifera: A tool for the reconstruction of surface water stratification, in: Fischer, G., Wefer, G. (Eds.), *Use of Proxies in Paleoceanography: Examples from the South Atlantic*. Springer, pp. 165–189.

Oppo, D.W., Fairbanks, R.G., 1989. Carbon isotope composition of tropical surface water during the past 22,000 years. *Paleoceanography* 4, 333–351. doi: 10.1029/PA004i004p00333

Pedro, J.B., Rasmussen, S.O., van Ommen, T.D., 2012. Tightened constraints on the time-lag between Antarctic temperature and CO<sub>2</sub> during the last deglaciation. *Clim. Past* 8, 1213–1221. doi: 10.5194/cp-8-1213-2012

Skinner, L.C., Fallon, S., Waelbroeck, C., Michel, E., Barker, S., 2010. Ventilation of the deep Southern Ocean and deglacial CO<sub>2</sub> rise. *Science* 328, 1147–1151. doi: 10.1126/science.1183627

Staffelbach, T., Stauffer, B., Sigg, A., Oeschger, H., 1991. CO<sub>2</sub> measurements from polar ice cores: more data from different sites. *Tellus B* 43, 91–96. doi: 10.1034/j.1600-0889.1991.t01-1-00003.x

Svensson, A., Andersen, K.K., Bigler, M., Clausen, H.B., Dahl-Jensen, D., Davies, S.M., Johnsen, S.J., Muscheler, R., Parrenin, F., Rasmussen, S.O., Röthlisberger, R., Seierstad, I., Steffensen, J.P., Vinther, B.M., 2008. A 60,000 year Greenland stratigraphic ice core chronology. *Clim. Past* 4, 47–57. doi: 10.5194/cp-4-47-2008

Veres, D., Bazin, L., Landais, A., Kele, H.T.M., Lemieux-Dudon, B., Parrenin, F., Martinerie, P., Blayo, E., Blunier, T., Capron, E., Chappellaz, J., Rasmussen, S.O., Severi, M., Svensson, A., Vinther, B.M., Wolff, E., 2013. The Antarctic ice core chronology (AICC2012): an optimized multi-parameter and multi-site dating approach for the last 120 thousand years. *Clim. Past* 9, 1733–1748. doi: 10.5194/cpd-8-6011-2012

**Table S1.** *G. bulloides*  $\delta^{18}\text{O}$  and  $\delta^{13}\text{C}$  of core-top sediments in the South Atlantic obtained by H.-W. Hubberten and H.-S. Niebler (Alfred-Wegener-Institute, Germany)

| Location | Latitude | Longitude | Elevation (m) | $\delta^{18}\text{O}$ (permil PDB) | $\delta^{13}\text{C}$ (permil PDB) | Fraction              |
|----------|----------|-----------|---------------|------------------------------------|------------------------------------|-----------------------|
| PS1759-1 | -50.165  | 5.755     | -3793         | 3.234                              | 0.705                              | 250-315 $\mu\text{m}$ |
| PS1759-1 | -50.165  | 5.755     | -3793         | 3.173                              | 0.219                              | 200-250 $\mu\text{m}$ |
| PS1775-5 | -50.952  | -7.503    | -2523         | 3.271                              | 0.417                              | 250-315 $\mu\text{m}$ |
| PS1779-3 | -50.3992 | -14.0803  | -3574         | 3.031                              | 0.682                              | 250-315 $\mu\text{m}$ |
| PS1779-3 | -50.3992 | -14.0803  | -3574         | 3.081                              | 0.454                              | 200-250 $\mu\text{m}$ |
| PS2103-2 | -51.3292 | -3.3243   | -2947         | 2.566                              | 0.337                              | 250-315 $\mu\text{m}$ |
| PS2103-2 | -51.3292 | -3.3243   | -2947         | 2.469                              | -0.042                             | 200-250 $\mu\text{m}$ |
| PS2104-1 | -50.7425 | -3.2118   | -2592         | 3.176                              | 0.472                              | 250-315 $\mu\text{m}$ |
| PS2341-1 | -55.6155 | -57.6353  | -4247         | 2.510                              | 0.701                              | 200-250 $\mu\text{m}$ |
| PS2341-1 | -55.6155 | -57.6353  | -4247         | 2.507                              | 1.261                              | 250-315 $\mu\text{m}$ |
| PS2341-1 | -55.6155 | -57.6353  | -4247         | 2.724                              | 0.472                              | 200-250 $\mu\text{m}$ |
| PS2341-1 | -55.6155 | -57.6353  | -4247         | 2.041                              | 0.802                              | 250-315 $\mu\text{m}$ |
| PS2341-1 | -55.6155 | -57.6353  | -4247         | 2.293                              | 1.126                              | 250-315 $\mu\text{m}$ |
| PS2341-1 | -55.6155 | -57.6353  | -4247         | 2.353                              | 1.359                              | 250-315 $\mu\text{m}$ |
| PS2341-1 | -55.6155 | -57.6353  | -4247         | 2.325                              | 0.838                              | 200-250 $\mu\text{m}$ |
| PS2343-1 | -55.165  | -58.0917  | -3281         | 2.217                              | 0.563                              | 250-315 $\mu\text{m}$ |
| PS2343-1 | -55.165  | -58.0917  | -3281         | 1.865                              | 0.118                              | 200-250 $\mu\text{m}$ |
| PS2343-1 | -55.165  | -58.0917  | -3281         | 1.898                              | 0.059                              | 200-250 $\mu\text{m}$ |
| PS2343-1 | -55.165  | -58.0917  | -3281         | 1.944                              | 0.066                              | 250-315 $\mu\text{m}$ |
| PS2351-1 | -53.765  | -58.8867  | -575          | 2.219                              | 0.560                              | 250-315 $\mu\text{m}$ |
| PS2351-1 | -53.765  | -58.8867  | -575          | 2.075                              | 0.113                              | 200-250 $\mu\text{m}$ |
| PS2351-1 | -53.765  | -58.8867  | -575          | 1.956                              | 0.225                              | 250-315 $\mu\text{m}$ |
| PS2351-1 | -53.765  | -58.8867  | -575          | 2.031                              | 0.304                              | 200-250 $\mu\text{m}$ |
| PS2352-1 | -53.7367 | -58.9033  | -1033         | 2.077                              | 0.616                              | 250-315 $\mu\text{m}$ |
| PS2352-1 | -53.7367 | -58.9033  | -1033         | 2.094                              | 0.363                              | 200-250 $\mu\text{m}$ |
| PS2352-1 | -53.7367 | -58.9033  | -1033         | 2.107                              | 0.625                              | 250-315 $\mu\text{m}$ |
| PS2352-1 | -53.7367 | -58.9033  | -1033         | 1.597                              | -0.121                             | 200-250 $\mu\text{m}$ |
| PS2353-1 | -53.7367 | -58.9033  | -1033         | 2.613                              | 0.559                              | 250-315 $\mu\text{m}$ |
| PS2353-1 | -53.7367 | -58.9033  | -1033         | 2.116                              | 0.426                              | 200-250 $\mu\text{m}$ |
| PS2353-2 | -53.6067 | -58.9767  | -1916         | 1.691                              | 0.230                              | 200-250 $\mu\text{m}$ |
| PS2353-2 | -53.6067 | -58.9767  | -1916         | 2.126                              | 0.664                              | 250-315 $\mu\text{m}$ |

**Table S2.** Age-depth markers in MD07-3076Q obtained from calibrated radiocarbon dates and the stratigraphic alignment of abundance lows of *N. pachyderma* (s.) (%Nps) with maxima of the first derivative of the EDC δD record

| Depth (cm) | Age (a BP) | Method <sup>1</sup>  |
|------------|------------|--|
| 1.5        | 1203       | <sup>14</sup> C, Skinner et al., 2010                                      |
| 5.5        | 1625       | <sup>14</sup> C, Skinner et al., 2010                                      |
| 9.5        | 2240       | <sup>14</sup> C, Skinner et al., 2010                                      |
| 15.5       | 3297       | <sup>14</sup> C, Skinner et al., 2010                                      |
| 21.5       | 4734       | <sup>14</sup> C, Skinner et al., 2010                                      |
| 25.5       | 5658       | <sup>14</sup> C, Skinner et al., 2010                                      |
| 31.5       | 6543       | <sup>14</sup> C, Skinner et al., 2010                                      |
| 35.5       | 7018       | <sup>14</sup> C, Skinner et al., 2010                                      |
| 41.5       | 8455       | <sup>14</sup> C, Skinner et al., 2010                                      |
| 45.5       | 9353       | <sup>14</sup> C, Skinner et al., 2010                                      |
| 49.5       | 10003      | <sup>14</sup> C, Skinner et al., 2010                                      |
| 53.5       | 10569      | <sup>14</sup> C, Skinner et al., 2010                                      |
| 55.5       | 10847      | <sup>14</sup> C, Skinner et al., 2010                                      |
| 59.5       | 11277      | <sup>14</sup> C, Skinner et al., 2010                                      |
| 61.5       | 11538      | <sup>14</sup> C, Skinner et al., 2010                                      |
| 63.5       | 11842      | <sup>14</sup> C, Skinner et al., 2010                                      |
| 67.5       | 12536      | <sup>14</sup> C, Skinner et al., 2010                                      |
| 73.5       | 13043      | <sup>14</sup> C, Skinner et al., 2010                                      |
| 77.5       | 13405      | <sup>14</sup> C, Skinner et al., 2010                                      |
| 85.5       | 14362      | <sup>14</sup> C, Skinner et al., 2010                                      |
| 89.5       | 14670      | <sup>14</sup> C, Skinner et al., 2010                                      |
| 91.5       | 14792      | <sup>14</sup> C, Skinner et al., 2010                                      |
| 95.5       | 14938      | <sup>14</sup> C, Skinner et al., 2010                                      |
| 99.5       | 15205      | <sup>14</sup> C, Skinner et al., 2010                                      |
| 109.5      | 16590      | <sup>14</sup> C, Skinner et al., 2010                                      |
| 113.5      | 17113      | <sup>14</sup> C, Skinner et al., 2010                                      |
| 117.5      | 17578      | <sup>14</sup> C, Skinner et al., 2010                                      |
| 119.5      | 17802      | <sup>14</sup> C, Skinner et al., 2010                                      |
| 121.5      | 18006      | <sup>14</sup> C, Skinner et al., 2010                                      |
| 125.5      | 18381      | <sup>14</sup> C, Skinner et al., 2010                                      |
| 133.5      | 19042      | <sup>14</sup> C, Skinner et al., 2010                                      |
| 137.5      | 19403      | <sup>14</sup> C, Skinner et al., 2010                                      |
| 145.5      | 20512      | <sup>14</sup> C, Skinner et al., 2010                                      |
| 161.5      | 22881      | <sup>14</sup> C, Skinner et al., 2010                                      |
| 173.5      | 24743      | <sup>14</sup> C, Skinner et al., 2010                                      |
| 187.5      | 26234      | <sup>14</sup> C, Skinner et al., 2010                                      |
| 197.5      | 27380      | <sup>14</sup> C, Skinner et al., 2010                                      |
| 232.0      | 30062      | %Nps aligned to $\delta(\text{EDC } \delta\text{D})/\delta t$ (this study) |
| 294.9      | 34188      | %Nps aligned to $\delta(\text{EDC } \delta\text{D})/\delta t$ (this study) |
| 333.7      | 36072      | %Nps aligned to $\delta(\text{EDC } \delta\text{D})/\delta t$ (this study) |

|       |       |  |
|-------|-------|--|
| 380.5 | 39384 | %Nps aligned to $\delta(\text{EDC } \delta\text{D})/\delta t$ (this study) |
| 429.3 | 41680 | %Nps aligned to $\delta(\text{EDC } \delta\text{D})/\delta t$ (this study) |
| 459.1 | 43571 | %Nps aligned to $\delta(\text{EDC } \delta\text{D})/\delta t$ (this study) |
| 509.5 | 47004 | %Nps aligned to $\delta(\text{EDC } \delta\text{D})/\delta t$ (this study) |
| 606.5 | 54517 | %Nps aligned to $\delta(\text{EDC } \delta\text{D})/\delta t$ (this study) |
| 685.6 | 60002 | %Nps aligned to $\delta(\text{EDC } \delta\text{D})/\delta t$ (this study) |
| 739.8 | 65325 | %Nps aligned to $\delta(\text{EDC } \delta\text{D})/\delta t$ (this study) |
| 760.1 | 66741 | %Nps aligned to $\delta(\text{EDC } \delta\text{D})/\delta t$ (this study) |
| 772.5 | 68026 | %Nps aligned to $\delta(\text{EDC } \delta\text{D})/\delta t$ (this study) |

<sup>1</sup>Calibrated calendar ages of the core section between 0-98 cm have been accidentally misreported in the Supporting Information of the original publication. Correct ages are listed here.

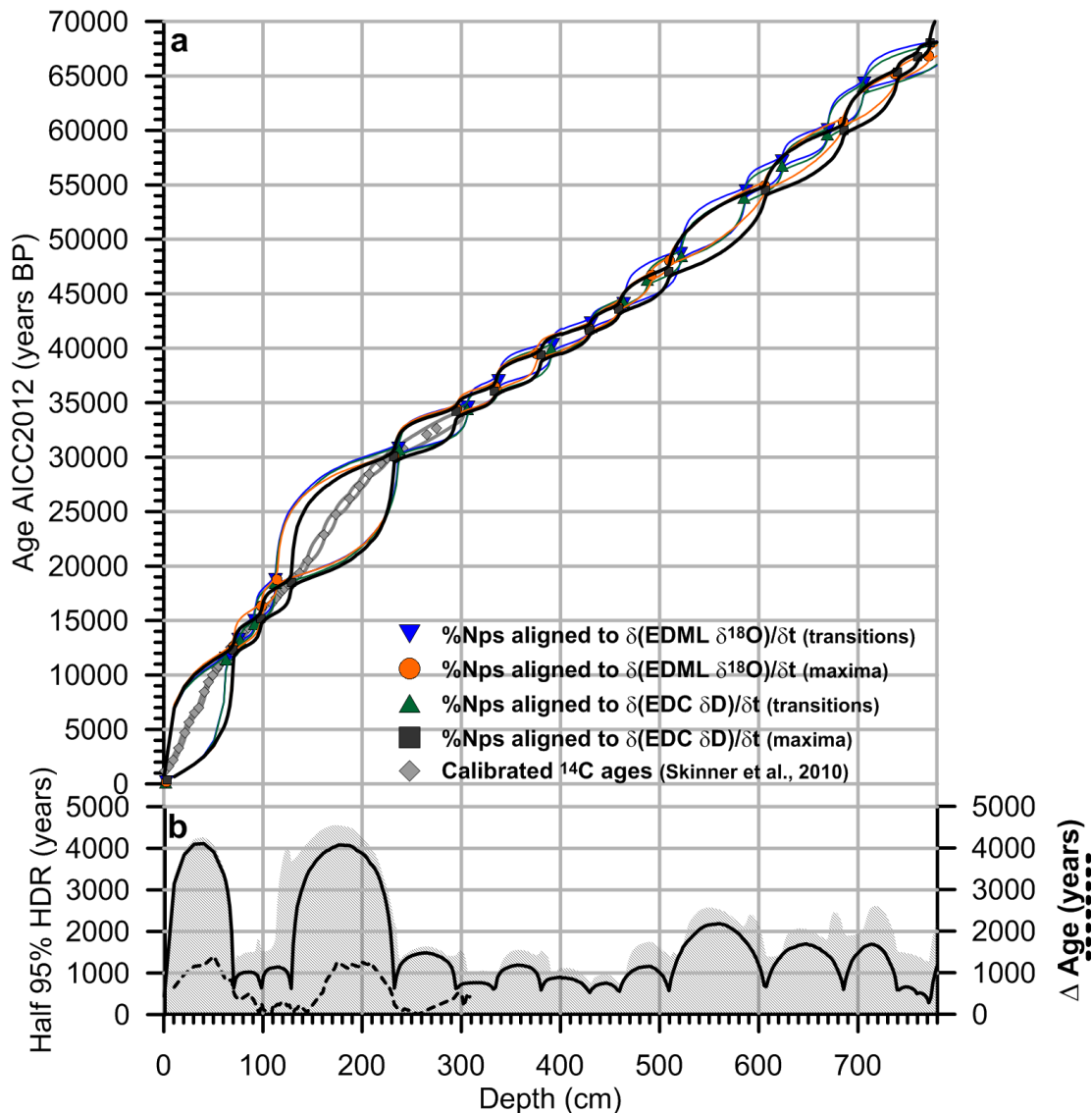


**Fig. S1.** a) Age-depth markers in sediment core MD07-3076Q derived from calibrated radiocarbon ages (grey diamonds) (Skinner et al., 2010) and the stratigraphic alignment of variations in the abundance of *N. pachyderma* (s.) (%Nps) with the first derivative of the EPICA Dome C (EDC) δD and the EPICA Dronning-Maud-Land (EDML)  $\delta^{18}\text{O}$  records on the AICC2012 age scale (Veres et al., 2013) (the alignment of %Nps lows with the maximum rate of change of the EDC and EDML records is respectively shown as dark squares and orange circles; the alignment of %Nps with the rate of change of Antarctic temperature observed in the EDC and EDML ice cores in transitional phases are shown as green triangles and blue inverse triangles, respectively), envelopes highlight the resulting age model uncertainties (95% high posterior density region, HDR) calculated with the Bayesian statistical software BCHRON (Haslett and Parnell, 2008), b) half of the 95% HDR region of the chronology that is based on the alignment of %Nps lows with maxima of the first derivative of the EDC δD record (black) in comparison to the maximum half 95% HDR region obtained from all alignment approaches (hatched); the difference in absolute ages obtained from the %Nps-based chronology and the radiocarbon-based age model, where they overlap, is shown as stippled line

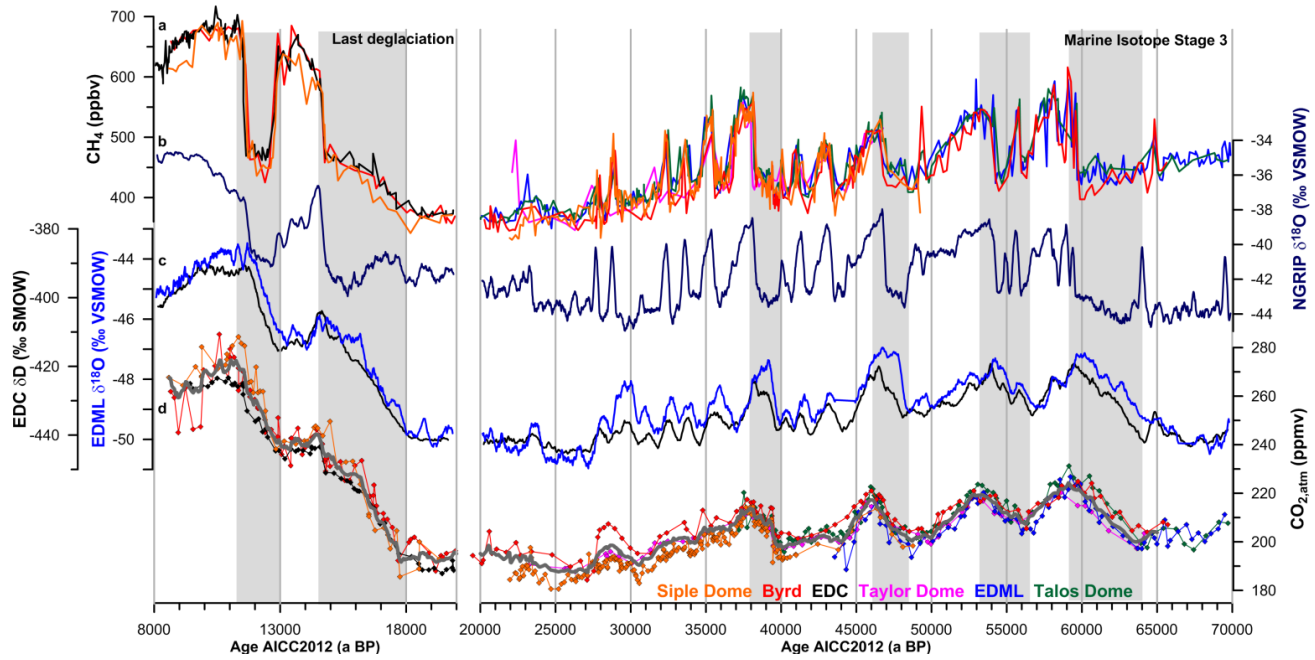


**Fig. S2.** Compilation of high-resolution atmospheric  $\text{CH}_4$  and  $\text{CO}_2$  data of the last 70000 years: a)  $\text{CH}_4$  concentrations reconstructed from Siple Dome (Ahn and Brook, 2014; Brook et al., 2005), EPICA Dome C (EDC) (Monnin et al., 2001), EPICA Dronning Maud Land (EDML) (EPICA Community Members, 2006), Taylor Dome (Brook et al., 2000), Talos Dome (Buiron et al., 2012) and the Byrd (Blunier and Brook, 2001) ice cores, b)  $\delta^{18}\text{O}$  variability of the Greenland NGRIP ice core on the GICC05 age scale (Svensson et al., 2008), which is equivalent to the AICC2012 age scale (Veres et al., 2013), c)  $\delta\text{D}$  (grey) and  $\delta^{18}\text{O}$  (blue) of the EDC and EDML ice cores (EPICA Community Members, 2006; Jouzel et al., 2007) on the AICC2012 age scales (Veres et al., 2013), d) atmospheric  $\text{CO}_2$  ( $\text{CO}_{2,\text{atm}}$ ) concentrations reconstructed from Siple Dome (Ahn and Brook, 2014; Ahn et al., 2004), EDC (Monnin et al., 2001), EDML (Bereiter et al., 2012; Lüthi et al., 2010), Talos Dome (Bereiter et al., 2012), Taylor Dome (Indermühle et al., 2000) and the Byrd ice core (Ahn and Brook, 2008; Blunier and Brook, 2001); the mean  $\text{CO}_{2,\text{atm}}$  is marked as a grey line; grey bars show intervals of rising  $\text{CO}_{2,\text{atm}}$